Case Studies in Construction Materials 19 (2023) e02521

Contents lists available at ScienceDirect

Case Studies in Construction Materials

journal homepage: www.elsevier.com/locate/cscm

Experimental Study into the Mechanical Properties of Plastic Concrete: Compressive Strength Development over Time, Tensile Strength and Elastic Modulus

David Alós Shepherd [a,b,*,1], Frank Dehn [a,b]

[a] Materials Testing and Research Institute Karlsruhe (MPA Karlsruhe), Gotthard-Franz-Str. 2/3, 76131 Karlsruhe, Germany
[b] Institute of Concrete Structures and Building Materials (IMB), Gotthard-Franz-Str. 3, Bldg. 50.31, 76131 Karlsruhe, Germany

ARTICLE INFO

Keywords:
Plastic concrete
Compressive strength
Elastic modulus
fib MC 2020
Splitting tensile strength
Time development

ABSTRACT

Plastic Concrete is a low-strength ($f_{cm,28d} \leq$ 1.0 MPa), low-stiffness, impervious concrete used for cut-off wall construction in earthen dams. To date, there has been no systematic study on the effect of mix design on the long-term time development of the mechanical properties (compressive strength, tensile strength, and elastic modulus) of Plastic Concrete. Therefore currently no Plastic Concrete specific constitutive law for cut-off wall design exists. The present study closes this gap. Ten Plastic Concrete mixes with two bentonite-cement ratios and three types of sodium bentonite were produced. Fresh concrete workability tests were performed for all mixes. Compressive strength tests were performed at ages 28 d, 56 d, 91 d and four years. Splitting tensile strength and elastic modulus tests were performed at 28 days. The workability results show a good linear correlation between slump and flow table tests. Plastic Concrete's compressive strength development over time is notably slower than that of ordinary concrete, and a new time development model following *fib* MC 2020 is established using a fitted s_C coefficient. The splitting tensile strength shows an overall good, linear correlation with compressive strength, with an approximate ratio of 0.135. Furthermore, the elastic modulus $E_{C,S}$ according to EN 12390-13 concrete tests show significantly higher elastic modulus than the available data, and a model approximation for the elastic modulus $E_{C,S}$ as a function of compressive strength is also provided. Overall, this study provides the first Plastic Concrete specific mechanical property models, confirming the critical role mix design plays on Plastic Concrete's short and long-term mechanical properties. Thus, the developed models enable a more realistic Plastic Concrete cut-off wall design and provide an important basis for future research.

1. Introduction

1.1. Background

Due to a significantly ageing infrastructure, dam remediation and repair is of increasing importance worldwide. Earthen dams, commonly used for hydropower generation, levees or flood retention basins, also show significant ageing, and their safety is of utmost

* Corresponding author at: Materials Testing and Research Institute Karlsruhe (MPA Karlsruhe), Gotthard-Franz-Str. 2/3, 76131 Karlsruhe, Germany.
E-mail address: david.alosshepherd@kit.edu (D. Alós Shepherd).
[1] 0000-0001-9966-735

https://doi.org/10.1016/j.cscm.2023.e02521
Received 27 August 2023; Received in revised form 26 September 2023; Accepted 30 September 2023
Available online 2 October 2023

importance for nearby urban areas. Therefore, earthen dams must also be remediated, whereby the most common solution for the remediation of earthen dams and levees is the design and construction of cut-off walls [1,2]. The planned cut-off wall, generally constructed as a slurry-trench wall [3], is extended into an underlying impervious stratum [4] and filled with a support fluid to stop the excavated trench from collapsing. The trench is then usually backfilled using the tremie method [1,2], whereby a wide range of backfill materials exist, with growing interest in Plastic Concrete due to the materials' suitable characteristics [1].

Plastic Concrete is hereby characterised by a high deformation capacity under load. This, in turn, decreases both rupture probability and crack opening width, reducing the probability of a permeability increase in the cut-off wall [1,2,5]. Plastic Concrete is, similar to ordinary concrete, composed of cement, water, aggregate, additions and admixtures, however, in differing proportions [1]. Most notably, Plastic Concrete is produced with a very high w/c-ratio (w/c $\geq$ 3.0) and water-binding additions (e.g. bentonite) to ensure fresh concrete stability and hereby obtain a highly ductile and impermeable material [1].

Despite its indisputably beneficial material properties, the mechanical behaviour of Plastic Concrete still needs to be widely studied [1]. Currently, the design of cut-off walls considers Plastic Concrete to be a linear-elastic material, with a defined compressive strength at 28 days [6], since no specific constitutive law for Plastic Concrete exists, which could account for the time development of the mechanical properties of Plastic Concrete [1]. This is not least due to the scarcely available systematic data in the literature, whereby the compressive strength, tensile strength and elastic modulus cannot be correlated from one mix design. The lack of a specific constitutive law also generally incurs higher cement contents than technically necessary, ensuring the strength criteria are permanently met in the linear-elastic design [6]. Thus, the material's full potential is only partially used and the inherent sustainability advantages do not come into effect [6]. The resulting increased costs may also significantly impede using Plastic Concrete in developing countries [7,8]. Therefore, in the following subsections, the current understanding of the mechanical behaviour of Plastic Concrete is summarised.

1.1.1. Compressive strength

In literature, various studies have tested the unconfined compressive strength of Plastic Concrete with varying mix design [9–12–15,16,17]. The studies show a gradual decline in Plastic Concrete strength with increasing w/c-ratio. However, since bentonite absorbs water into its structure, reducing the readily available water for cement hydration, the effective w/c-ratio is likely smaller. In literature there is no reference to the contending behaviour of cement and bentonite for the available water and possible interaction mechanisms in Plastic Concrete. In addition, compressive strength results are also dependent on the chosen loading speed and testing standard [18,19]. They must therefore be considered carefully to achieve measurable and precise data, avoiding any loading-speed induced effects [18,19]. The existing literature, however, does not systematically address these influencing parameters when studying the material behaviour of Plastic Concrete [1].

Furthermore, Plastic Concrete batching and casting are also of utmost importance for the material's performance. Various possibilities exist for batching [20,21], where a pre-hydrated bentonite slurry is most commonly added to cement and aggregates before mixing [1]. Especially the preparation of the bentonite slurry has a significant impact on Plastic Concrete performance, whereby the few available studies recommend a long mixing time with a high-RPM mixer [22] to ensure sufficient bentonite mixing. Regarding swelling time, current literature does not find significant differences in Plastic Concrete's performance with varying swelling times [21, 23].

Even though most reference testing for standard concrete is conducted at 28 days, it is common knowledge that the strength of concrete continues to increase beyond this mark. The knowledge of the long-term strength development of Plastic Concrete is of utmost importance since cut-off walls are constructed for design periods far exceeding 50 years. In addition, the water load application on cut-off walls occurs far beyond the 28-day mark; therefore, long-term strength development is essential to ensure accurate and realistic cut-off wall design. The curing speed of concrete is primarily influenced by factors such as water-cement ratio, type of cement and cement strength class [24]. For the latter, higher cement strength classes generally lead to faster strength development due to cement's increased fineness [18,24]. Code models like the *fib* Model Code 2010 [25] or *fib* Model Code 2020 [26] can be used to estimate the time function of concrete strength development (see Subsection 4.3). It is also known that, generally, the tensile strength develops faster than the corresponding compressive strength [26,27]. Literature data has, however, already shown that Plastic Concrete's compressive strength development is far slower than ordinary concrete, with a significant compressive strength increase beyond the 28-day mark [1,9,11,15,17]. This should be accounted for in Plastic Concrete cut-off wall design with a material-specific time development model, which, however, currently does not exist, and will therefore be studied in this paper.

1.1.2. Tensile strength

In concrete design, the uniaxial tensile strength (f_{ct}) is as important as the uniaxial compressive strength. For standard concrete, the uniaxial tensile strength is typically estimated to be 10% of the unconfined compressive strength f_{cu} [18]. However, this f_{ct}/f_{cu}-ratio is not constant and may decrease with increasing time and compressive strength f_{cu} [18,28]. Furthermore, the ratio is affected by the aggregate type, aggregate grading, curing conditions, and the type of tensile test performed [18,27].

According to *fib* MC 2010 [25], in turn based on the model by Heilmann [27,29], the tensile strength f_{ctm} can be estimated from the characteristic compressive strength f_{ck} following Equation (1) for concrete grades $\leq$ C50 [25].

$$f_{ctm} = 0.3 \cdot (f_{ck})^{2/3} \tag{1}$$

However, for a Plastic Concrete sample with a characteristic compressive strength f_{ck} of 1.5 MPa, this would incur in a mean tensile strength f_{ctm} of 0.39 MPa, suggesting a f_{ctm}/f_{ck}-ratio of 0.26, unlikely for Plastic Concrete samples. Heilmann however shows that the

factor 0.3 in Equation (1) may vary depending on the type of test used [27,29] and will therefore be studied in more detail in the present study.

On the other hand *fib* MC 2020 [26] suggests a new model, described in Equation (2).

$$f_{ctm} = 1.8 \cdot ln(f_{ck}) - 3.1 \tag{2}$$

However, this model is not applicable to Plastic Concrete since a negative tensile strength would be calculated for a characteristic compressive strength f_{ck} of 1.5 MPa. Therefore this model is not further pursued in the present study.

The tensile strength of concrete can be studied with various test methods. Most commonly, and due to the simple testing procedure, the so-called splitting tensile strength (also called "Brazilian test") standardised in EN 12390–6 [30] or ASTM C496 [31] is used. The splitting tensile test is usually performed on cylinders with a height-to-diameter ratio of 2, with smaller samples generally exhibiting higher strength [27]. It should be noted that tensile strength tests generally exhibit a higher standard deviation than compressive strength tests [18,24]. However, the sample size has a smaller influence on splitting tensile tests than on other tensile tests due to the stress induction mechanism and sample failure pattern [18,24]. The conversion factor α_{sp} for splitting tensile strength to uniaxial tensile strength for ordinary concrete is disputed in literature [24,28] and varies widely in existing international codes [26]; *fib* MC 2020 [26] therefore recommends using a conversion factor $\alpha_{sp} = 1.0$.

For Plastic Concrete, little research has been carried out on tensile strength. Gao et al. [32] performed splitting tensile strength tests on cubes with two sample sizes, showing a good correlation between the compressive strength and the tensile strength. Kahl et al. [33] studied a wide range of Plastic Concrete mixes at different ages using 6 in by 12 in cylinders, also finding a clear correlation between the achievable splitting tensile strength and the selected mix design. Finally Kayser and schulz [34] performed few splitting tensile strength tests on 10 cm by 20 cm cylinders of hardened cement-bentonite slurries with different bentonites. In conclusion, the present paper must systematically study the tensile-to-compressive strength ratio, specifically for Plastic Concrete, and establish a new model for this purpose.

1.1.3. Elastic modulus

In Plastic Concrete cut-off wall design, the target elastic modulus should be similar to the surrounding soil's, and not exceed five times the latter, to ensure compatibility within the earthen dam [1,35]. The elastic modulus of concrete is hereby primarily determined by the elastic moduli of its components [18,19]. Similarly to ordinary concrete, the elastic modulus of Plastic Concrete increases with increasing compressive strength and thus with decreasing w/c-ratio or increasing cement content [1]. In literature, various studies have investigated the elastic modulus of Plastic Concrete [10,11,13,14,16,17,36]. Still, as reported by the authors in [1], the testing procedure used has a major influence on the test results. This is primarily due to the varying definitions of elastic modulus underlying the individual testing procedures and the different sample deformation measurement techniques used [1].

In concrete technology, elastic modulus testing is performed according to EN 12390-13 [37] or ASTM C469 [38], whereby the sample deformation is measured using dial gauges or LVDTs applied directly to the samples. On the other hand, geotechnical testing standards such as EN ISO 17892-7 [39] or ASTM D2166 [40] generally use machine displacement to obtain specimen deformation in a load-displacement curve. In addition, the definition of elastic modulus differs depending on the selected testing procedure and is, therefore, not directly comparable. Overall, the elastic modulus obtained through concrete technology testing procedures is expected to be higher than that from geotechnical standards. With the available data, the elastic modulus of Plastic Concrete based on geotechnical standards can be assumed to be in the range of 300–1500 MPa [1].

However, in the literature, no elastic modulus data is available for Plastic Concrete samples based on concrete technology testing procedures. Therefore, the present study aims to close this gap.

1.2. Focus & research questions

In conclusion, the existing literature fails to systematically study the effect of mix design, especially w/c-ratio, bentonite content and type, on the long-term time development of the mechanical properties of Plastic Concrete. In addition, no Plastic Concrete specific time development model exists to estimate the concrete strength development beyond the 28-day mark. Furthermore, Plastic Concrete's compressive-to-tensile strength ratio remains unclear, with limited data showing no distinct pattern. In addition, all elastic modulus data available to date has been obtained using the load-displacement curve of geotechnical compressive strength tests and not based on direct sample measurement techniques. However, these measurements also account for testing machine deformation and fail to study solely material behaviour as measured in situ on the samples. The successful application of elastic modulus testing according to EN 12390-13 [37] specifically on Plastic Concrete samples, remains to be reported.

Therefore, this paper aims to critically study the effect of Plastic Concrete mix design, especially bentonite content and type, on its mechanical properties. The focus also lies on the long-term time development (up to 4 years) of compressive strength of Plastic Concrete and the development of a Plastic Concrete specific compressive strength time development model. In addition, the fresh concrete properties of Plastic Concrete are tested using two separate testing methods (slump and flow table test) to establish a correlation between the two. In addition, splitting tensile tests are conducted for the corresponding compressive strength tests to determine a tensile-to-compressive strength ratio. Finally, the elastic modulus of Plastic Concrete is tested for the first time following EN 12390-13 [37] and provides realistic elastic modulus data for varying mix designs. The developed models are of key importance to ensure a more accurate and realistic Plastic Concrete cut-off wall design.

2. Materials and methods

2.1. Materials

The present study studied bentonite-based Plastic Concrete mixes consisting of cement, bentonite, aggregates and water, with a high w/c-ratio, as described in subsection 1.1.

2.1.1. Cement and bentonite

In the present study, a German OPC cement CEM I according to EN 197–1 [41] was used. Three activated sodium bentonites from different European deposits were used to study the corresponding effect on Plastic Concrete performance. These were Bentonil CV15, Bentonil WW4 and Tixoton, all produced and provided by CLARIANT Deutschland GmbH, were used. No further supplementary cementitious materials (SCMs) were added.

The chemical composition of the source materials, as determined through X-ray fluorescence analysis (XRF), is given in Table 1. The physical characteristics of the source materials are given in Table 2. In Table 3, the mineralogical composition, as determined through XRD, as well as the cation exchange capacity (CEC), as determined through Cu-trien method according to [42,43], of the bentonites used are shown.

2.1.2. Aggregates and water

The aggregates used were a combination of local Rhine sand and Rhine gravel from Graben-Neudorf, Germany. The maximum aggregate size was $d_{max} = 8$ mm, in line with considerations from literature [1]. The particle size distribution is shown Table 4 and lies between control sieve curve A8 and B8 according to DIN 1045–2 [44].

The mixing water used was mains water from Karlsruhe, previously tempered to 20°C, and in line with the requirements according to EN 1008 [45]. No admixtures were used since currently available PCE-based admixtures interact (negatively) with clay, rendering these ineffective [46].

2.2. Methods

2.2.1. Experimental setup and mix design

As mentioned in section 1, no systematic study has investigated the time development of compressive and tensile strength of Plastic Concrete. In addition no Plastic Concrete specific concrete models exist in literature. Therefore, this study investigates Plastic Concrete's compressive strength change over time as well as studying the splitting tensile strength of Plastic Concrete at 28 days with varying mix design. In addition, the fresh properties of concrete were tested. Finally, the elastic modulus of Plastic Concrete is determined in accordance with EN 12390-13 [37] at 28 days. A timeline of the experimental tests is shown in Fig. 1.

To further understand the changes in Plastic Concrete mechanical strength, the bentonite type and the bentonite content were varied. Three activated sodium bentonites were used (see Subsubsection 2.1.1). The bentonite to cement ratio (b:c-ratio) was varied between 1:1.5 and 1:6. An overview of the varying mix design factors and the corresponding designation of the mixes used for compressive strength, splitting tensile strength and fresh concrete testing is given in Table 5. For elastic modulus testing, only the 1:2 and 1:3 mixes were used.

It is well established in the literature that the bentonite to cement ratio (b:c-ratio), as well as the w/c-ratio, have a crucial influence on the material strength obtained for a Plastic Concrete mix [1,47]. With a Plastic Concrete target compressive strength between 0.5 and 2.5 MPa at 28 days, and based on previous studies conducted by the authors [1,23], a Plastic Concrete mix with 100 kg/m^3 of cement and a w/c-ratio of 4.0 was used. The mix designs of Plastic Concrete used in this study are shown in Table 6.

2.2.2. Concrete batching and fresh concrete testing

Based on the experimental setup developed in Subsubsection 2.2.1, and following considerations in [1], the Plastic Concrete mixes in this study were produced by combining the dry components (cement and aggregate) with the (pre-hydrated) bentonite slurry. Since no standardised batching procedure exists for Plastic Concrete, this process is described in more detail.

The bentonite slurry was produced in a batch suspension mixer type SC-20-K from MAT Mischanlagentechnik GmbH (Immenstadt, Germany). This mixer reaches a rotational speed of approx. 3000 rpm (50 Hz) and has a nominal power of 5.5 kW. The capacity of the mixer is approximately 20 litres. The batch suspension mixer was filled with 20 litres of water, and bentonite was added evenly to avoid clump formation [21]. The components were then mixed in the mixer for 6 min to achieve a homogeneous bentonite slurry [1,22]. The slurry was then filled into buckets through a discharge pipe on the mixer. The 24-hour swelling process

Table 1
Chemical composition of the cement and bentonites used, corrected by LoI.

		CaO	SiO_2	Al_2O_3	MgO	Fe_2O_3	Others	LoI
CEM I	(m.-%)	61.8	22.2	5.2	2.9	2.4	3.6	2.7
CV15	(m.-%)	2.3	59.8	12.0	1.9	2.2	3.4	15.7
WW4	(m.-%)	4.0	50.6	16.7	3.1	3.8	4.1	17.8
Tixoton	(m.-%)	3.9	49.2	17.5	2.5	5.3	5.4	18.2

Table 2
Physical characteristics of the cement and bentonite source materials used.

	PSD			density			specific surface
	$d_{10\%}$* (μ m)	$d_{50\%}$*	$d_{90\%}$*	no-dry (g/cm^3)	60°C	105°C	Blaine (cm^2/g)
CEM I	1.52	17.20	55.30	3.10	–	–	3.477
CV15	1.20	7.13	38.34	2.40	2.72	2.79	–
WW4	0.93	4.75	39.90	2.54	2.72	2.86	–
Tixoton	1.97	16.78	57.19	2.57	2.72	2.78	–

* Determination in water with $Na_4P_2O_7$

Table 3
Mineralogical composition determined by XRD and CEC of the bentonites used.

	CV15	WW4	Tixoton
Quartz	X	X	X
Carbonate (mainly calcite)	X	X	X
Illite / Mica (di)			X
Montmorillonite	X	X	X
Plagioclase	X	X	X
K-feldspar		X	X
CEC ($cmol^+/kg$)	61	88	65

"X" marks where the minerals are present

Table 4
Particle size distribution of aggregates used.

Sieve size	(mm)	0.125	0.25	0.5	1	2	4	8
Sieve passing	(m.-%)	0.5	8.8	21.0	30.2	40.0	63.2	97.2

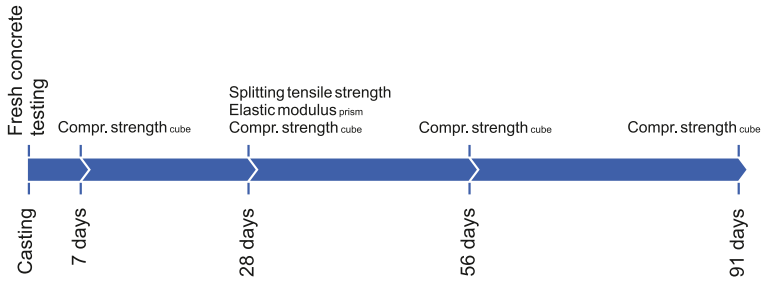

Fig. 1. Timeline of the experimental testing carried out in this study.

Table 5
Overview of the varying mix design factors and corresponding designation of the mix designs used.

b:c-ratio	Bentonite Type		
	Bentonil CV15	Bentonil WW4	Tixoton
1:1.5	C1:1.5	W1:1.5	T1:1.5
1:2	C1:2	W1:2	T1:2
1:3	C1:3	W1:3	–
1:4	C1:4	–	–
1:6	C1:6	–	–

and storage also took place in these buckets, which were placed in a climate-controlled room with an air temperature of 20°C and a relative humidity of 65%.

The fresh Plastic Concrete was mixed using two different mixers depending on the concrete batch size. For batches up to 50 litres, a Zyklos ZZ 75 EH concrete mixer from Pemat Mischtechnik GmbH (Freisbach, Germany) was used. This mixer has a nominal

Table 6
Mix design of Plastic Concrete.

	Mix I (kg/m^3)	Mix II (kg/m^3)	Mix III (kg/m^3)	Mix IV (kg/m^3)	Mix V (kg/m^3)
Cement	100.0	100.0	100.0	100.0	100.0
Water	400.0	400.0	400.0	400.0	400.0
Bentonite	066.6	050.0	033.3	025.0	016.7
Sand (0–2 mm)	556.6	562.9	569.2	572.3	575.5
Gravel (2–8 mm)	873.5	883.4	893.3	898.2	903.1
b/c-ratio	1:1.5	1:2	1:3	1:4	1:6

power of 3.3 kW, a rotational speed of approximately 70 rpm and a capacity of 75 litres. For larger batches up to 240 litres, a pan concrete mixer from Teka Maschinenbau GmbH (Edenkoben, Germany) was used. This mixer has a nominal power of 15 kW, a rotor speed of approximately 17 rpm and a capacity of 375 litres. In addition, the ambient temperature in the laboratory was approximately 20°C.

First, sand, gravel and cement were placed in the mixer drum and premixed for one minute. After that the bentonite slurry, with a prior 24 h swelling time, was added to the mixer drum. The Plastic Concrete was then mixed for 5 min until a homogeneous concrete mix was obtained. This is in line with the most common mixing procedure for Plastic Concrete [1] and also used in previous studies by the authors [23].

The finalised fresh concrete is then tested, with slump test according to EN 12350-2 [48] and flow table test according to EN 12350-5 [49] being performed immediately after mixing. Following on, fresh concrete density according to EN 12350-6 [50] and air content according to EN 12350-7 [51] were measured.

Thereafter, part of the concrete was cast into standard cubic (a=200 mm) and cylinder (l=300 mm, d=150 mm) steel moulds according to EN 12390-1 [52] and vibrated with a rod shaker with a 120 Hz frequency. In addition, the remaining part of the concrete was cast into standard 40 × 40 × 160 mm^3 steel prism moulds according to EN 196–1 [53] and vibrated on a shaking table with a 50 Hz frequency for 30 s. All samples were then stored in the moulds for 72 h (due to the low early age strength) at 20°C under plastic foil and wet jute to avoid desiccation of samples following EN 12390-2 [54]. After this, the samples were demoulded and placed under water at 20°C until testing.

2.2.3. Compressive strength testing

Most commonly, the compressive strength of concrete is determined according to EN 12390-3 [55] using cubic samples with an edge length of 150 mm. However, due to Plastic Concrete's very low strength properties, the minimum testing load of standard concrete uniaxial testing machines is not reached at Plastic Concrete sample failure. Therefore, cubes with an edge length of 200 mm were used, to increase test area and thus testing load. For any given age and mix, three cubes were tested. The cast cubes were removed from the water bath curing and surface dried using a cloth towel. The compressive strength was not tested thoroughly in compliance to EN 12390-3 [55] since the loading speed was reduced in line with the low strength requirements of Plastic Concrete. The loading speed was set to 0.05 MPa/s for all samples, as similarly described in DIN 4093 [56] for the testing of strengthened soil samples.

2.2.4. Splitting tensile strength testing

Furthermore, the tensile strength of specimens was studied using the splitting tensile test according to EN 12390-6 [30]. The tested cylinders were 300 mm in length and 150 mm in diameter. For any given age and mix, three cylinders were tested. The cast cylinders were removed from the water bath curing and surface dried using a cloth towel. Due to Plastic Concrete's very low strength properties, the splitting tensile strength was not tested thoroughly according to EN 12390-6 [30] since the loading speed had to be reduced. The loading speed was hereby set to 350 N/s (equivalent to 0.005 MPa/s).

2.2.5. Elastic modulus testing

Most commonly, the elastic modulus of concrete is determined according to EN 12390-13 [37] using cylinder samples with 150 mm diameter and 300 mm in length. However, due to Plastic Concrete's very low strength, standard concrete uniaxial testing machines are inadequate to test Plastic Concrete samples due to the minimum testing load. Therefore a specialised testing machine Zwick 010 from the manufacturer ZwickRoell GmbH & Co. KG (Ulm, Germany) was used. This electrical AC servomotor universal testing machine has a maximum load capacity of 10 kN and crosshead speed ranging between 0.0005 mm/min to 1000 mm/min, making the machine suitable for testing low-strength samples such as Plastic Concrete. The cast prisms were removed from the water bath curing and surface dried using a cloth towel. For any given age and mix, three prisms were tested. The prisms were placed vertically in the testing machine (testing cross-section 40 × 40 mm^2), and two oppositely placed DD1 strain transducers on a quick-action clamping device were used for sample deformation measurement. Thereafter the stabilised elastic modulus test according to EN 12390–13, procedure B [37] was performed. The loading speed was set to 0.01 MPa/s for all samples, with a pre-load stress of 0.06 MPa. Once elastic modulus testing was finalised, the clamping device with the strain transducers was removed from the samples, and the corresponding compressive strength was tested following EN 12390-3 [55] with an identical loading speed of 0.01 MPa/s. Deformation of the samples was hereby measured using the crosshead displacement.

3. Results

3.1. Fresh concrete results

As mentioned in Subsubsection 2.2.2, fresh concrete tests were performed on the concrete batches produced. Fig. 2 provides an overview of the fresh concrete workability results. In Fig. 3, the air content and fresh concrete density results are shown.

The results in Fig. 2 clearly show that an increase in bentonite content, i.e. increasing b:c-ratio, incurs lower Plastic Concrete workability, likely due to the water-binding capacity of bentonite and inline with results from other research [7,23,57–59]. It should be noted that mixes C1:6 and T1:2 (marked with * and hatched) displayed some minimal segregation and are therefore not considered for future analysis. In addition, at a constant b:c-ratio, the bentonite type used has a significant effect on concrete workability [23]. Finally, the results display a good correlation between the flow table and slump test results and will be further discussed in Subsection 4.1.

From Fig. 3, it becomes apparent that no clear correlation between b:c-ratio and the obtained air content exists, likely due to the known high scattering of air content test results. On the other hand, as would be expected for the selected mix designs (see Table 6), an increase in b:c-ratio incurs a lower concrete density, due to the intrinsic volumetric replacement of (heavier) aggregates with (lighter) bentonite. Nonetheless, variations in test execution can also affect the test results obtained, of particular importance with high b:c-ratio mixes, where a correct placement and compaction of the Plastic Concrete samples cannot be guaranteed due to the decreased workability.

3.2. Compressive strength results

As mentioned in Subsubsection 2.2.3, three cubes were tested on compression in accordance with EN 12390-3 [55] for every point in time and selected mix. In Fig. 4, the results from compressive strength tests at 28 days in dependence of the b:c-ratio are shown, whereby each point represents the mean value of three samples with its corresponding standard deviation.

Fig. 4 shows that the compressive strength at 28 days lies between 0.33 MPa and 0.79 MPa, aligning with the results expected in literature for the chosen mix [1,23,47]. Moreover, the results show a clear correlation between compressive strength and the b:c-ratio used, with compressive strength increasing with a higher bentonite content, due to a decreasing effective w/c-ratio [23,60,61]. The two mixes displayed in Fig. 4 with hollow symbols are not in line with this trend due to slight concrete segregation (see also Fig. 2) and subsequent concrete bleeding, increasing compressive strength of the remaining samples. Therefore it can be assumed that the b:c-ratio and compressive strength, for a given bentonite type, have a positive correlation.

The overall strength is, however, also dependent on the bentonite type used, for which literature is currently inconclusive. The cation exchange capacity (CEC), and thus bentonites' water absorption capacity, could affect the compressive strength of samples. However, as shown in Table 3, the CEC of WW4 bentonite is highest, but the samples exhibit lower strength than CV15 samples, contradicting this theory. In Fig. 5, the results from compressive strength testing are shown over time, whereby each point represents the mean value of three results, with corresponding standard deviation.

Fig. 5 shows that the compressive strength increases steadily from 28 days onwards. The compressive strength at 28 days lies between 0.58 MPa and 0.80 MPa, aligning with the results expected in literature for the chosen mix design [1,23,47]. In addition, the strength increase beyond 28 days is far greater than that of ordinary concrete due to Plastic Concrete's far higher w/c-ratio and reported slower cement hydration [20,61]. The compressive strength of Plastic Concrete samples tested here increases by approximately 30–50% between 28 days and 91 days due to continuous cement hydration and subsequent pore refinement over time [23]. These results will be further discussed in Subsection 4.3.

Moreover, a clear correlation between compressive strength and the b:c-ratio is visible, with the compressive strength of mixes with a 1:1.5 ratio lying above that of 1:3 mixes. Through a higher bentonite content in the mix, a lower effective w/c-ratio is incurred,

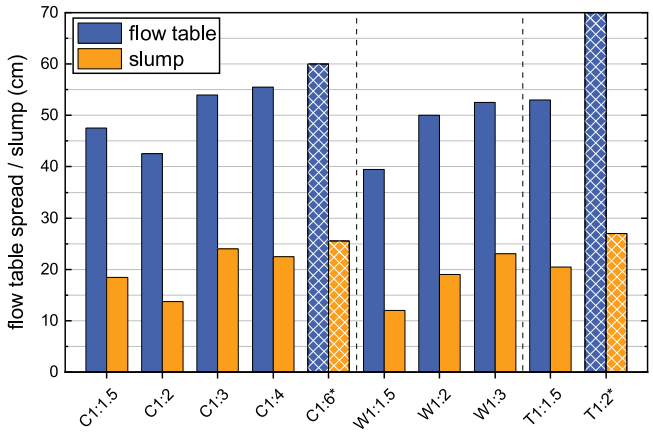

Fig. 2. Fresh concrete workability test results of all mixes.

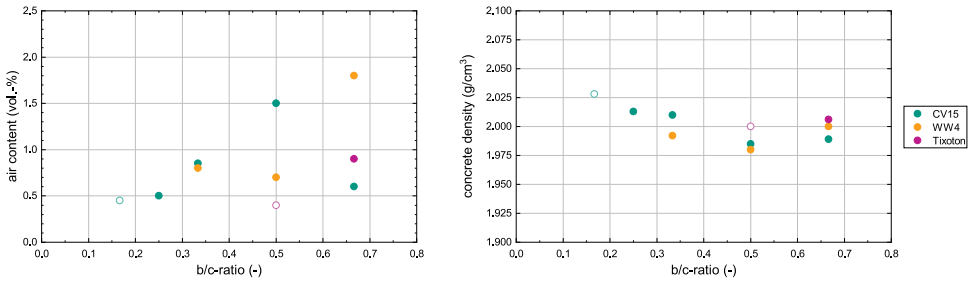

Fig. 3. Fresh concrete air content (left) and density (right) test results of all mixes.

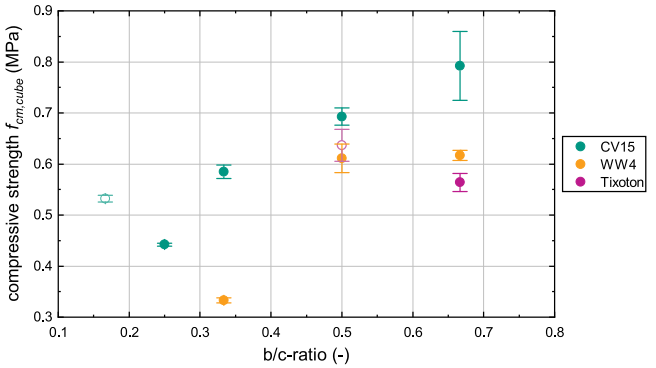

Fig. 4. Mean compressive strength (with standard deviation) of three cube samples (a = 200 mm) in dependence of b:c-ratio of Plastic Concrete at 28 days.

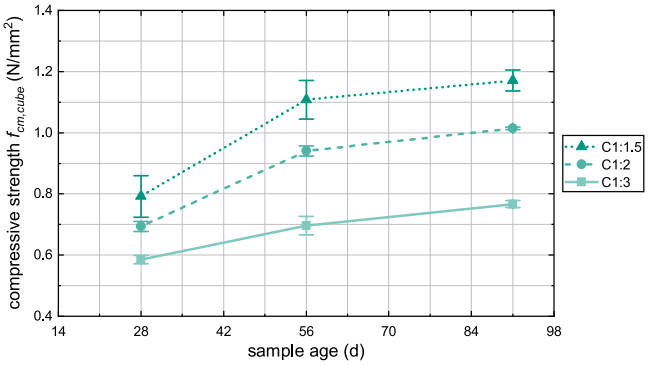

Fig. 5. Mean compressive strength (with standard deviation) of three cubes over time in dependence of Plastic Concrete mix design.

allowing for a more dense cementitious matrix and, in turn, increasing the compressive strength [23,60,61].

3.3. *Splitting tensile strength results*

As described in Subsubsection 2.2.3, the splitting strength was tested according to EN 12390-6 [30] on three cylinders per mix design. In Fig. 6, the results from splitting tensile strength testing at 28 days in dependence of the b:c-ratio are shown, whereby each point represents the mean value of three samples with its corresponding standard deviation.

The results show that the splitting tensile strength at 28 days lies between 0.048 MPa and 0.103 MPa, aligning with the results expected in literature for the chosen mix [1]. Moreover, the results show some correlation between splitting tensile strength and the b:c-ratio used, with splitting tensile strength increasing with a higher bentonite content. However, the standard deviation of splitting tensile strength test results is far higher than that of compressive strength, as known from literature [24]. From the displayed results it remains inconclusive whether a dependency of splitting tensile strength on the bentonite type used exists and will be further studied in subsection 4.4.

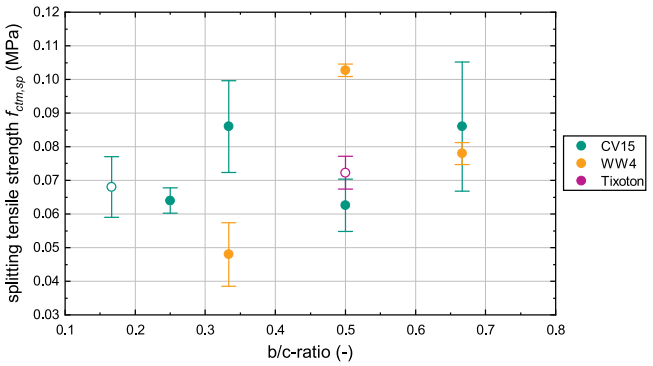

Fig. 6. Mean splitting tensile strength (with standard deviation) of three cylinder samples (l = 300 mm, d = 150 mm) in dependence of b:c-ratio of Plastic Concrete at 28 days.

3.4. Elastic modulus results

Elastic modulus tests according to EN 12390-13, procedure B [37] were performed on prism samples as described in Subsubsection 2.2.5. Thereafter, the corresponding compressive strength was tested following EN 12390-3 [55]. In Fig. 7, the elastic modulus $E_{C,S}$ test results are shown over the corresponding compressive strength, whereby each point represents one tested prism sample.

The results show that, as expected, an increase in compressive strength incurs in higher elastic modulus of Plastic Concrete samples. It is also apparent that neither bentonite type nor b:c-ratio significantly impact the achievable elastic modulus. Due to prism sample slenderness (h/d=4), most compressive strength results underestimate the correct compressive strength since the samples partially displayed shear failure. The results of the elastic modulus testing will be further discussed in Subsection 4.5.

4. Discussion

4.1. Slump and flow table correlation

As shown in Subsection 3.1, a positive correlation between the slump and flow table test results for Plastic Concrete seems to exist. Despite concrete being measured under different conditions with both tests (self-weight vs compaction), both test methods are suitable for testing high workability mixes [18,62]. To further analyse this correlation, the results from this study as well as a further study by the authors in [23], are plotted in Fig. 8 with the slump test results being displayed over flow table tests results.

It can be seen that, as expected, slump increases with increasing flow table spread, similar to results in ordinary concrete [63]. In addition, this trend occurs independently of the type of bentonite used. The results from this study have a marginally lower spread than those from [23]. The Guide to Tremie Concrete for Deep Foundations [62] states that the flow table test has a lower sensitivity while using dynamic impacts that may alter the obtained results. However, since no superplasticizing admixtures were used for the mix design the achieved workability is lower than standard tremie concrete and is therefore more appropriate for flow table testing. This is also in line with the limits defined in DIN Fachbericht 100 [64] where the presented results lay within the recommended limits for flow table testing (34–62 cm). The slump results lay slightly above the recommended limits (1–21 cm) [64].

Although Norvell et al. [57] suggest that concrete flowability correlates to the cation exchange capacity (CEC) of the bentonites used, the results presented in Fig. 2 and in Fig. 8 do no support this thesis, since nearly identical CECs of CV15 and Tixoton bentonite (see Table 3) incur in significantly different flow table results, despite identical mix designs. Fernandes et al. [59] describe a positive

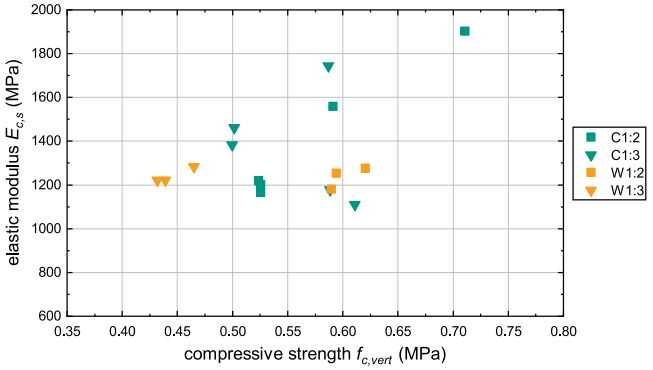

Fig. 7. Elastic modulus $E_{C,S}$ over compressive strength in dependence of Plastic Concrete mix design at 28 days.

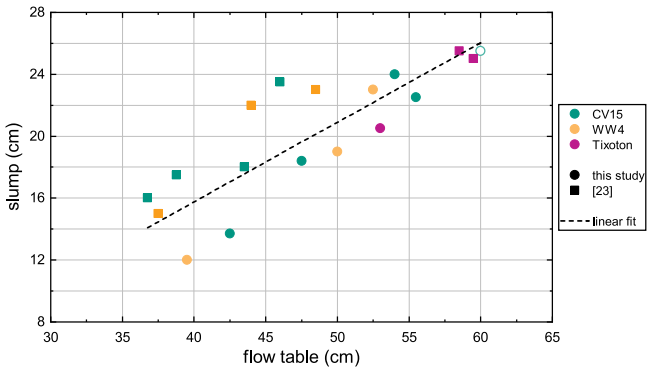

Fig. 8. Correlation between flow table and slump tests results for all mixes from this study and [23].

correlation between the moisture content (defined as the ratio by mass of water to solids) and the slump test results. However, in the present study, all mixes have an identical moisture content and thus, the varying workability of the mixes cannot be ascribed to this factor.

The linear trend of these results can be fitted and an approximate inclination of 0.52 is obtaine dwithin the tested data range displayed, i.e. that an increase in flow table spread of 10 cm incurs a 5.2 cm larger slump, inline with results presented in [62]. The coefficient of determination R^2 is only 0.646 due to the high, expected deviation of the fresh concrete test results. This high deviation is inherent with the applied fresh concrete test, reported to be ± 4 cm for flow table test results [62]. However, the overall trend can be accurately described with the displayed curve, where slump *s* correlates with flow table results *ft* according to Equation (3).

$$s = 0.52 \cdot (ft - 40\ \text{cm}) + 16\ \text{cm} \tag{3}$$

Future research should also measure the slump flow and slump flow velocity of Plastic Concrete mixes [62], since these results may display lower deviation for fresh tremie concrete properties.

4.2. *Influence of sample size and batching on compressive strength*

In this study, all compressive strength tests were conducted on cube samples with an edge length of 200 mm (as described in subsubsection 2.2.3). This, in turn, incurs a far more significant material consumption. Since the Plastic Concrete studied here has a maximum aggregate size d_{max} of 8 mm, it may therefore be more expedient to use prisms halves for compressive strength determination. Thus, within the scope of a previous study by the authors in [23], cube samples were cast to compare compressive strength

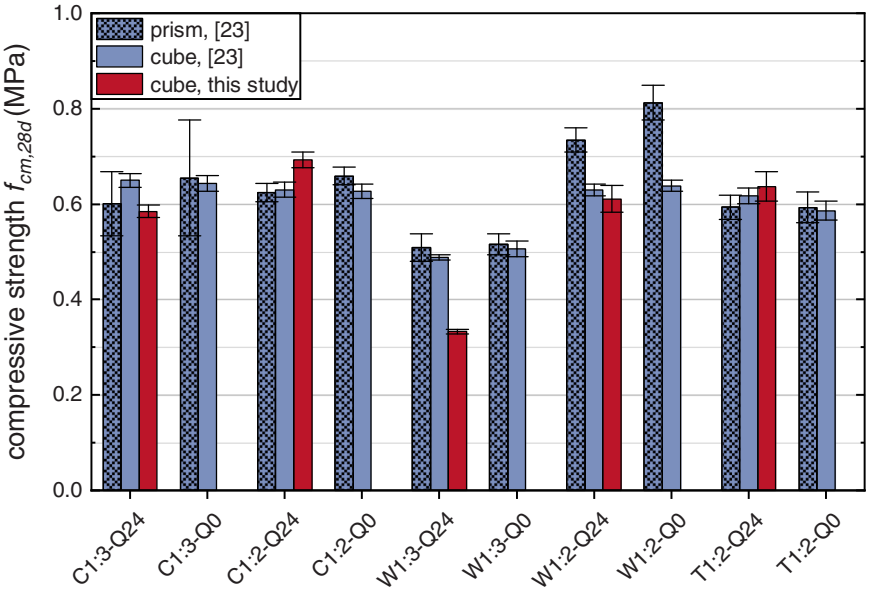

Fig. 9. Comparison of compressive strength of prism (40 × 40 mm^2) and cube samples (200 × 200 mm^2) from [23], with cube samples (200 × 200 mm^2) from this study, at 28 days.

results with prism halve samples. In addition, all samples from both studies were produced using the same batch of cement and bentonite, as well as aggregates from the same deposit, thus reducing the possible material scattering to a minimum. In Fig. 9, the results from this study and [23] are shown, whereby the strength is displayed over the corresponding mix design.

From this data it becomes apparent that cube samples have an overall repeatability since both studies provide similar compressive strength results. In addition, for most mix designs, the compressive strength of prism halve samples is close to that of cube samples, with both results lying within the standard deviation of one another. The data also shows that the standard deviation is approximately three times higher for the prism (0.0397 MPa) than cube (0.0143 MPa) samples, as would be expected due to the size and failure concentration effect based on the Weibull theory [18]. An average coefficient of the mean cube strength and prism strength can be calculated ($f_{cm,cube}/f_{cm,prism}$), with cubes strength being on average 0.963 × prism strength, in line with the expected theoretical correlation in literature [18]. Moreover, due to the chosen mix design (see subsubsection 2.2.1), the Plastic Concrete mixes tested in this study can all be considered water-dominated mixes [47]. Thus, the sample size has a less significant effect on compressive strength results than in standard concrete since cement particles are far further apart than in ordinary concrete, providing the same sample failure pattern (cross tensile failure) occurs. All in all, it can therefore be ascertained that the compressive strength of prism samples (40 × 40 mm^2) is approximately identical to that of cube samples (200 × 200 mm^2), despite higher standard deviation for prism samples. These results indicate that future research on Plastic Concrete compressive strength can be conducted using prism samples (providing $d_{max} \leq 8$ mm) due to the significant saving in the concrete volume needed for testing without significant influence on the compressive strength results. Furthermore, the results presented here should be further confirmed with more available research data in future.

4.3. Compressive strength development over time

In Subsection 3.2 the compressive strength results have been reported. However, the significant increase in compressive strength beyond the 28-day mark should be discussed in more detail.

For strength development of standard concrete, the *fib* Model Code 2010 [25] gives an approximation for the time function of the concrete strength development β_{cc} as a function of a cement-strength-class-dependant coefficient s and concrete age t, as shown in Equation (4).

$$\beta_{cc}(t) = \exp\left(s \cdot \left[1 - \left(\frac{28}{t}\right)^{0.5}\right]\right) \tag{4}$$

Few studies have examined the long-term strength of Plastic Concrete mixtures [9,11,15,17,65]. Therefore the results from this study as well as from [9,11,15,17] are shown in Fig. 10, where the relative compressive strength increase beyond 28 days ($f_{cm}(t)/f_{cm,28d}$) is shown as a function of time. For comparison, the *fib* MC 2010 model is also shown for a coefficient s of 0.20 and 0.38, respectively.

From Fig. 10, it becomes visible that the strength development over time is far more significant for Plastic Concrete samples than the *fib* MC 2010 predicts. The results from this study show a strength increase of 30–50% between 28 d and 91 d. It can also be seen that the compressive strength increase also clearly depends on the achievable compressive strength at 28 days and the w/c-ratio used, with a more substantial increase, the lower the corresponding compressive strength. From these results, changing the reference testing age for Plastic Concrete samples also seems expedient.

In *fib* MC 2020 [26], the time development function $\beta_{cc}(t)$ has been further extended in comparison to *fib* MC 2010 [25], whereby a different reference age t_{ref} can be further accounted for, as shown in Equation (5). If t_{ref} is set to 28 days, Equation (5) simplifies to Equation (4).

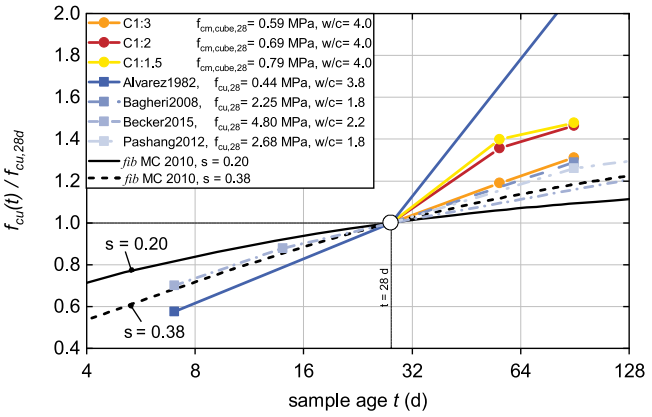

Fig. 10. Compressive strength of Plastic Concrete samples over time for this study and [9,11,15,17], with $t_{ref} = 28$ d.

$$\beta_{cc}(t) = \exp\left\{ s_C \cdot \left[1 - \left(\frac{t_{ref}}{t} \right)^{0.5} \right] \cdot \left(\frac{28}{t_{ref}} \right)^{0.5} \right\} \tag{5}$$

The s_C coefficient in *fib* MC 2020 [26] hereby depends on the speed of strength development and strength class of the selected concrete and has been updated in comparison to the s coefficient in *fib* MC 2010 [25]. For a compressive strength under 35 MPa according to Table 14.6–7 in [26,66] the s_C coefficient is selected to 0.3 (slow), 0.5 (normal) or 0.6 (slow) in accordance with corresponding strength development speed.

Therefore in Fig. 11 the results from the present study and [23] are plotted over time using a reference age t_{ref} of 91 days. In addition, the *fib* MC 2020 time development function with $s_C = 0.50$ coefficient is plotted.

The results show that due to the high w/c-ratio used, the strength development of Plastic Concrete is still significantly slower than the *fib* Model Code 2020 [26] estimates. Therefore, adapting this model for Plastic Concrete may seem reasonable, using a best-fit approximation of the s_C coefficient for the data available. The results show that a best-fit approximation with the *fib* MC 2020 curve for $s_C = 1.75$ ($R^2 = 0.82$) incurs in an underestimation of the strength development, most significantly for early age. Therefore, subdividing the approximation into two data sets, before and after 91 days, may be more expedient. The best-fit approximation for these two subdivided data sets is also shown in Fig. 11.

It can be seen that through the split, best-fit approximation, a better correlation with the data can be achieved, with the early age strength development approximated with $s_C = 0.65$ ($R^2 = 0.90$) and the later age strength development approximated with $s_C = 1.98$ ($R^2 = 0.97$) providing a far better correlation to the presented data. With this, the best-fit approximation for the s_C coefficient at t_{ref} = 91 days can be achieved as shown in Equation (6).

$$s_C = \begin{cases} 0.65 & t < 91 \text{ d} \\ 1.98 & t > 91 \text{ d} \end{cases} \tag{6}$$

Although unexpected, such a differentiated compressive strength development can make sense for Plastic Concrete. The initial, somewhat faster, strength development coincides with the initial cement hydration [23]. The long-term, slower compressive strength development is likely caused by another strength development mechanism, possibly through a cement-bentonite interaction or another reaction, for which literature currently provides no explanation. A previous study by the authors [23] confirmed that a significant pore refinement and compressive strength increase occurs between 91 days and 4 years; however, no evidence of a further interaction mechanism could be obtained. Another possibility would be that, with increasing sample age and cement hydration, some of the water bound by the bentonite becomes entrapped and therefore increase compressive strength during testing due to the incompressibility of water. However, microstructural evidence of this has not yet been studied.

Overall, with the results presented here, a better approximation of the long-term strength development can be achieved, ensuring a better and more realistic design of Plastic Concrete cut-off walls.

4.4. Tensile to Compressive Strength Ratio

In Subsection 3.2 and Subsection 3.3 the results of compressive and splitting tensile strength testing are shown. It is common knowledge in concrete technology that the tensile strength correlates with the compressive strength of specimens and can generally be approximated to 1/10 of the compressive strength [18,24] (see also Subsubsection 1.1.2). In Fig. 12, the results from this study are shown, whereby the splitting tensile strength is plotted over the corresponding compressive strength. For comparison, the approximated correlation between splitting tensile strength and compressive strength ($f_{ctm,\,psp} = 0.10 \cdot f_{cm}$) according to [18,24] is also shown.

From Fig. 12 it becomes apparent that Plastic Concrete also has an overall minimally higher tensile to compressive strength ratio than standard concrete, despite the overall higher standard deviation of splitting tensile test results [24].

In addition, some other authors have also published splitting tensile strength data for Plastic Concrete samples [32–34]. In Fig. 13, the splitting tensile strength is drawn over the corresponding compressive strength for the literature data [32–34] as well as the data from this study. In addition, best-fit modelling approaches following *fib* MC 2020 [26] / Heilmann [29] are shown, with the corresponding best-fit equation.

The results show a good correlation between splitting tensile strength and compressive strength results for Plastic Concrete samples over a broader range of compressive strength. The data furthermore lies above the expected ratio of 1/10. If a linear fit is applied, the splitting tensile can be approximated to Equation (7), with a ratio of 0.135. The coefficient of determination R^2 is 0.983, providing an overall excellent accordance for this data.

$$f_{ctm,sp} = 0.135 \cdot f_{cm} \tag{7}$$

Alternatively an approximation in line with *fib* MC 2020 [26]/Heilmann [29] can be calculated. The resulting approximation is shown in Equation (8). The coefficient of determination R^2 is 0.895, providing an overall good accordance for this data. However, as can be seen in Fig. 13, the tensile strength would be overestimated for low compressive strengths (0 - 1.5 MPa) and underestimated for higher compressive strengths (4 - 10 MPa) with this model.

$$f_{ctm,sp} = 0.179 \cdot f_{cm}^{2/3} \tag{8}$$

It should be noted that the specimen size, shape and testing standard used for the splitting tensile tests shown above are not

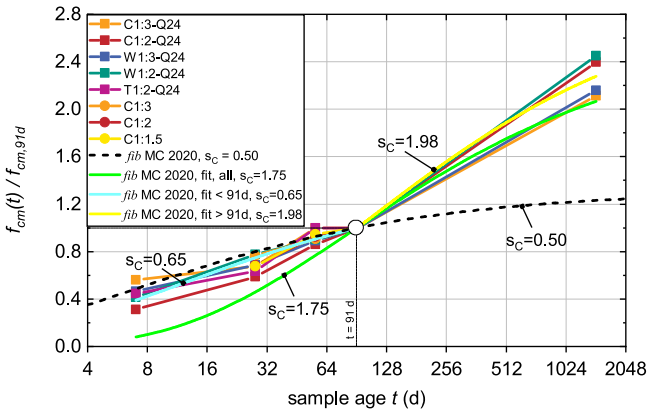

Fig. 11. Compressive strength of Plastic Concrete samples over time for this study and [23], as well as *fib* MC 2020 function, with $t_{ref} = 91$ d.

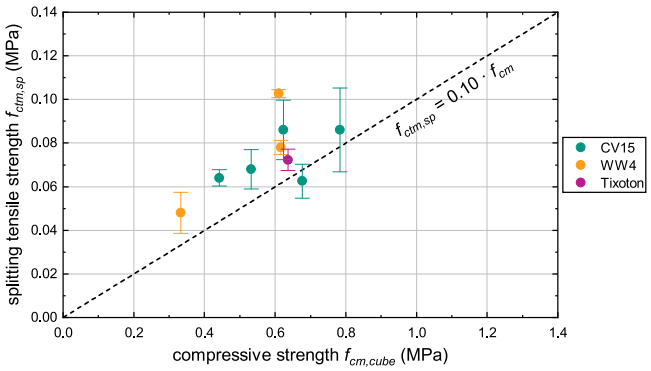

Fig. 12. Splitting tensile strength over compressive strength results at 28 days.

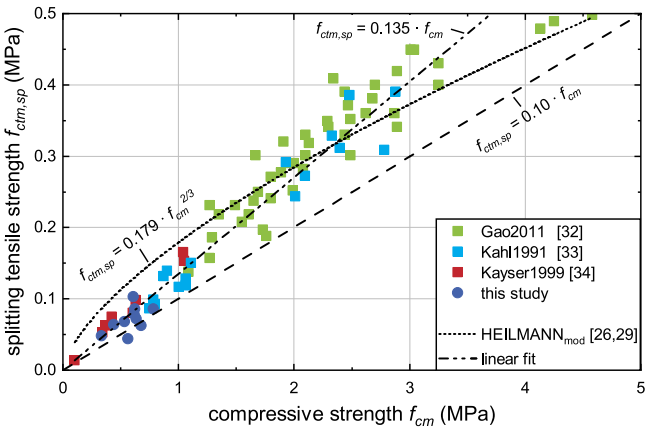

Fig. 13. Splitting tensile strength over compressive strength from this study and [32–34] as wells as modelling approximations in accordance with [26,29].

identical for all samples. The sample size and shape are known to have a small effect on splitting tensile strength results due to sample failure pattern [18,24], which might slightly affect model prediction accuracy. Nevertheless, it seems reasonable to adapt the models to the available data to better account for Plastic Concrete mechanical behaviour, since no material-specific tensile strength prediction model currently exists. In this sense, the linear prediction model (Equation (7)) currently provides the more accurate results, especially at very low compressive strengths, and should therefore be preferred and used for future Plastic Concrete cut-off wall design. In future, more data should be obtained to optimise the prediction accuracy of the proposed model.

4.5. Discussion of elastic modulus results

In Subsection 3.4 the results of the elastic modulus testing are shown. As described, the testing procedure used clearly influences the obtained elastic modulus, in-line with varying definitions of elastic modulus underlying the individual testing procedures [1] (see also Subsubsection 1.1.3). This is generally caused by the deviating deformation measurement techniques used [1]. Therefore, in the present study, the stabilised elastic modulus $E_{C,S}$ (hereinafter "stabilised modulus") was tested according to EN 12390-13, procedure B [37] with deformation measurement through two oppositely placed DD1 strain transducers on a quick-action clamping device. In addition, during subsequent compressive strength testing, the sample deformation was measured using the testing machines' cross-head displacement. A load-displacement curve is obtained with the latter, which can be further used to analyse sample deformation. Based on the *fib* MC 2020 [26], the initial elastic modulus E_{ci} can be obtained as the maximum tangent slope of the load-displacement-curve (hereinafter "tangent modulus"). In addition, the secant elastic modulus E_{c1} can also be obtained as the secant modulus from the origin to the peak compressive stress (hereinafter "secant modulus"). In the present study, the origin is here established as the intersection of the tangent modulus and the displacement axis to remove any contact effects in the load-displacement curve. In Fig. 14, the results of the present study with the stabilised elastic modulus $E_{C,S}$, the tangent elastic modulus E_{ci} and the secant elastic modulus E_{c1} are shown against the corresponding compressive strength. In addition the available literature data reported in [1] and based on [10,11,13,14,16,17,36] is shown in grey.

From the results in Fig. 14 it becomes clear that the testing scheme, especially the deformation measurement technique, plays a crucial role in the obtained elastic modulus results. The stabilised elastic modulus $E_{C,S}$ lies far above the other elastic moduli due to the direct deformation measurement of the samples and, therefore, also represents the "real" material behaviour. This testing incurs the lowest overall deformation and, thus, the highest elastic modulus, especially since deformation measurement occurs only in the middle third of the sample. When fitting the results, a linear approximation between the stabilised elastic modulus $E_{C,S}$ and the compressive strength f_c provides the best approximation with a coefficient of determination R^2 of 0.975 and is shown in Equation (9).

$$E_{C,S} = 2385 \cdot f_c \tag{9}$$

The results also show that the secant modulus $E_{c,i}$ and the tangent modulus E_{c1} provide similar results and are, as expected, in line with the results shown in literature from geotechnical testing standards. The tangent modulus is consistently higher than the secant modulus, which relates to the secant modulus accounting for the higher, plastic deformation of the Plastic Concrete samples. The present results provide the first comprehensive study of the elastic modulus of Plastic Concrete samples and a pioneering comparison between various testing methods. The results show that the stabilised elastic modulus $E_{C,S}$ is approximately 5.5x higher than the tangent modulus E_{ci} determined through the load-deformation curve. This suggests that, to date, cut-off wall design significantly underestimates Plastic Concrete material stiffness. However, since Plastic Concrete should provide a similar stiffness to the surrounding soil [1,35], and the soil stiffness is established as the tangent modulus in a load-displacement curve (see subsubsection 1.1.3), the tangent modulus E_{ci} may be the most appropriate value for geotechnical cut-off wall design. This is not least because the settlement calculations, and thus the load transfer onto the cut-off wall, use soil stiffness (i.e. tangent modulus) as input parameters. Once the design loads are obtained, these can be used as input for the Plastic Concrete cut-off wall stress analysis and wall design. The stress analysis can then be performed following available concrete design codes, and the newly developed models from this study, using the stabilised elastic modulus $E_{C,S}$.

5. Conclusions

The present study aimed to determine the effect of Plastic Concrete mix design on its mechanical properties over time and develop appropriate models. In addition, the present study also aimed to model the tensile-to-compressive strength ratio specifically for Plastic

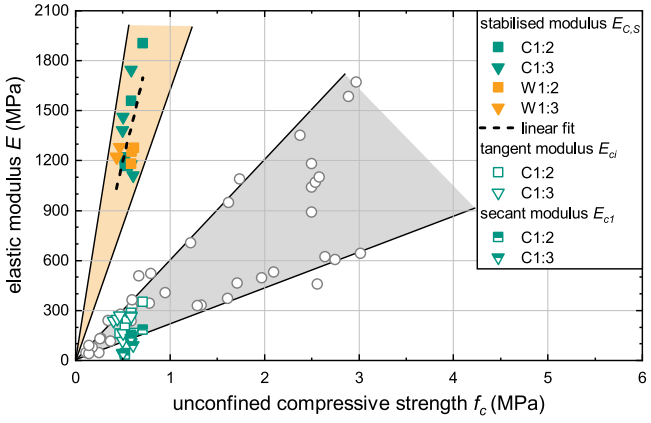

Fig. 14. Elastic modulus testing results ($E_{C,S}$, E_{ci}, E_{c1}) over corresponding unconfined compressive strength in comparison to literature results [1,10,11,13,14,16,17,36] (in grey) with varying mix design.

Concrete. Finally, the elastic modulus of Plastic Concrete was to be tested for the first time following EN 12390-13 [37] and related to the corresponding compressive strength.

This study's results show a good correlation between slump and flow table tests and can be estimated according to Equation (3). In addition, a wide range of compressive strength data is obtained for varying mix design and b:c-ratio. The compressive strength results for prism halve samples is shown to closely correlate to the corresponding cube strength, as seen in Fig. 9. Furthermore, a new time development model following *fib* MC 2020, specifically for Plastic Concrete, is developed exhibiting a significantly slower compressive strength increase over time, as described by the s_C coefficient in Equation (6). Furthermore, the splitting tensile strength shows an overall good, linear correlation with compressive strength with an approximate ratio of 0.135, as also shown in Fig. 13. Moreover, the elastic modulus $E_{C,S}$ concrete tests according to EN 12390-13 [37] show significantly higher elastic modulus than the available data (see Fig. 14), and a model approximation for the elastic modulus $E_{C,S}$ in dependence of compressive strength is given in Equation (9). All in all, this paper has provided a deeper insight into the understanding of Plastic Concrete's mechanical properties with varying mix design. In addition, the first Plastic Concrete specific mechanical property models have been developed,enabling a more realistic Plastic Concrete cut-off wall design and provide an essential basis for future research.

Future research should be carried out to explore the effect of the long-term strength increase in Plastic Concrete samples and further understand possible cement-bentonite interactions enhancing compressive and tensile strength time development models. In addition, further data should be acquired to adapt the newly developed models to a variation in source materials (e.g. CEM III or other SCMs) and also varying w/c-ratios. Finally, additional elastic modulus tests with varying mix design and sample ages should be performed to further develop the understanding of Plastic Concrete's elastic modulus. For this, novel measurement techniques such as digital image correlation (DIC) [67] could be explored, providing further insights into Plastic Concrete's mechanical behaviour.

Funding

This research did not receive any specific grant from funding agencies in the public, commercial, or not-for-profit sectors. The authors acknowledge support by the KIT-Publication Fund of the Karlsruhe Institute of Technology (KIT) for the settlement of the Article Publishing Charge.

CRediT authorship contribution statement

David Alós Shepherd: Conceptualization, Methodology, Investigation, Validation, Formal analysis, Writing – original draft, Writing – review & editing, Visualization, Project administration. **Frank Dehn**: Resources, Funding acquisition, Writing – review & editing.

Declaration of Competing Interest

The authors declare that they have no known competing financial interests or personal relationships that could have appeared to influence the work reported in this paper.

Data availability

Data will be made available on request.

Acknowledgements

The authors of this article would like to thank Clariant AG for providing the bentonite materials and MAT Mischanlagentechnik GmbH for providing the bentonite mixer. In addition, the authors would like to thank Ms. Anja Husel, Mr. Stefan Weber and Ms. Liv Wittkopf-Bertsch (IMB Karlsruhe/KIT) for their support during the testing campaign as part of their Bachelor's and Master's thesis. Furthermore, the authors thank Prof. Katja Emmerich and Dr. Eleanor Bakker (CMM Karlsruhe/KIT) for their help in CEC testing and their feedback regarding bentonite properties and behaviour.

References

[1] D. AlósShepherd, E. Kotan, F. Dehn, Plastic concrete for cut-off walls: a review, Constr. Build. Mater. 255 (2020), 119248, https://doi.org/10.1016/j.conbuildmat.2020.119248.
[2] D.A. Bruce (Ed.), Specialty Construction Techniques for Dam and Levee Remediation, CRC Press, Boca Raton, 2013.
[3] P.P. Xanthakos, Slurry walls, McGraw-Hill,, New York, 1979.
[4] U.S. Bureau of Reclamation Design Standards No. 13: Embankment Dam, Chapter 16: Cutoff Walls, Revision 14 (2014/07) (2014). ⟨https://www.usbr.gov/tsc/techreferences/designstandards-datacollectionguides/designstandards.html⟩.
[5] M. Ghazavi, Z. Safarzadeh, H. Hashemolhoseini, Response of plastic concrete cut-off walls in earth dams to seismic loading using finite element methods (Canadian Association for Earthquake Engineering (Ed.)). Proceedings of the 13th World Conference on Earthquake Engineering, Vancouver, 2004.
[6] K. Beckhaus, J. Kayser, F. Kleist, J. Quarg-Vonscheidt, D. Alós Shepherd, Design concept for sustainable cut-off walls made of highly deformable filling materials, in: R. Boes, P. Droz, R. Leroy (Eds.), Proceedings of the 12th ICOLD European Club Symposium 2023 (ECS 2023, Interlaken, Switzerland, 5-8 September 2023), CRC Press, Milton, 2023.

[7] F. Solomon, S.E. Ekolu, Strength behaviour of clay-cement concrete and quality implications for low-cost construction materials, in: M.G. Alexander, H.-D. Beushausen, F. Dehn, P. Moyo (Eds.), Concrete repair, rehabilitation and retrofitting III, Proceedings of the 3rd International Conference on Concrete Repair, Rehabilitation and Retrofitting (ICCRRR), Cape Town, South Africa, September 3rd - 5th 2012, CRC Press, Boca Raton, FL, 2012, pp. 1420–1425.
[8] M.L. Nehdi, Clay in cement-based materials: critical overview of state-of-the-art, Constr. Build. Mater. 51 (2014) 372–382, https://doi.org/10.1016/j.conbuildmat.2013.10.059.
[9] A.R. Bagheri, M. Alibabaie, M. Babaie, Reduction in the permeability of plastic concrete for cut-off walls through utilization of silica fume, Constr. Build. Mater. 22 (6) (2008) 1247–1252, https://doi.org/10.1016/j.conbuildmat.2007.01.024.
[10] J. Sadrekarimi, Plastic Concrete Mechanical Behaviour, J. Inst. Eng. India Civ. Eng. Div. 82 (FEV) (2002) 201–207.
[11] A. Becker, C. Vrettos, Laboruntersuchungen zum Materialverhalten von Tonbeton (in German), Bautechnik 92 (2) (2015) 152–160, https://doi.org/10.1002/bate.201400064.
[12] J.C. Evans, E.D. Stahl, E. Drooff, Plastic concrete cutoff walls, in: R.D. Woods (Ed.), Geotechnical practice for waste disposal 1987, Geotechnical Special Publications, ASCE, New York, 1987, pp. 462–472.
[13] S. Hinchberger, J. Weck, T. Newson, Mechanical and hydraulic characterization of plastic concrete for seepage cut-off walls, Can. Geotech. J. 47 (4) (2010) 461–471, https://doi.org/10.1139/T09-103.
[14] A. Mahboubi, A. Ajorloo, Experimental study of the mechanical behavior of plastic concrete in triaxial compression, Cem. Concr. Res. 35 (2) (2005) 412–419, https://doi.org/10.1016/j.cemconres.2004.09.011.
[15] Y. PashangPisheh, S.M. MirMohammadHosseini, Stress-strain behavior of plastic concrete using monotonic triaxial compression tests, J. Cent. South Univ. 19 (4) (2012) 1125–1131, https://doi.org/10.1007/s11771-012-1118-y.
[16] S. Kazemian, S. Ghareh, L. Torkanloo, To investigation of plastic concrete bentonite changes on it's physical properties, Procedia Eng. 145 (2016) 1080–1087, https://doi.org/10.1016/j.proeng.2016.04.140.
[17] L. Alvarez, J. Larenas, A. Bernal, J.A. Marin, Characteristics of the plastic concrete of the diaphragm wall of Convento Viejo Dam. International Commission On Large Dams (Ed.), 14th International Congress on Large Dams in Rio de Janeiro, Brazil, Vol. IV, 1982, pp. 371–389.
[18] A.M. Neville. Properties of Concrete, 5th edi., Pearson,, Harlow, 2011.
[19] H.-W. Reinhardt. Ingenieurbaustoffe (in German), 2nd ed., Ernst & Sohn,, Berlin, 2010.
[20] M.A. Fam, J.C. Santamarina, Study of clay-cement slurries with mechanical and electromagnetic waves, J. Geotech. Eng. 122 (5) (1996) 365–373, https://doi.org/10.1061/(ASCE)0733-9410(1996)122:5(365).
[21] M.A. Fadaie, M. Nekooei, P. Javadi, Effect of dry and saturated bentonite on plastic concrete, KSCE J. Civ. Eng. 23 (8) (2019) 3431–3442, https://doi.org/10.1007/s12205-019-0835-2.
[22] S. Adjei, S. Elkatatny, A. Al-Majed, Effect of bentonite prehydration time on the stability of lightweight oil-well cement system, Geofluids 2021 (2021) 1–8, https://doi.org/10.1155/2021/9957159.
[23] D. AlósShepherd, A. Bogner, J. Bruder, F. Dehn, Experimental Study into the Time Development of the Microstructural Properties of Plastic Concrete: Material Insights & Experimental Boundaries (In Review), Case Studies in Construction Materials (CSCM) (2023).
[24] P. Grübl, H. Weigler, S. Karl, Beton: Arten, Herstellung und Eigenschaften (in German). Handbuch fur Beton-, Stahlbeton- und Spannbetonbau, 2nd ed., Ernst & Sohn,, Berlin, 2001.
[25] International Federation for Structural Concrete (Ed.), fib Model Code for Concrete Structures 2010, 1st ed., Ernst & Sohn,, Berlin, 2013.
[26] International Federation for Structural Concrete (Ed.), fib Model Code for Concrete Structures 2020: Final Draft, May 2023, unpublished Edition, Lausanne, 2023/05.
[27] H.W. Reinhardt, Factors affecting the tensile properties of concrete, in: J. Weerheijm (Ed.), Understanding the tensile properties of concrete, Woodhead Publishing series in civil and structural engineering, Woodhead Publishing, Oxford, 2013, pp. 19–51, https://doi.org/10.1533/9780857097538.1.19.
[28] V. Malárics, Ermittlung der Betonzugfestigkeit aus dem Spaltzugversuch an zylindrischen Betonproben (in German): Dissertation, Vol. 69 of Karlsruher Reihe Massivbau, Baustofftechnologie, Materialprüfung, KIT Scientific Publishing,, Karlsruhe, 2011.
[29] H.G. Heilmann, Relations between tensile and compressive strength of concrete (in German), Beton 19 (2) (1969) 68–70.
[30] Comité Européen de Normalisation, EN 12390–6:2010–09 - Testing hardened concrete - Part 6: Tensile splitting strength of test specimens (German version).2023.
[31] ASTM International, ASTM C496/C496M-17 - Test Method for Splitting Tensile Strength of Cylindrical Concrete Specimens.2023.
[32] D.Y. Gao, S.Q. Song, L.M. Hu, Relationships of Strengths and Dimensional Effect of Plastic Concrete, Adv. Mater. Res. 306 307 (2011) 1029–1037, https://doi.org/10.4028/www.scientific.net/AMR.306-307.1029.
[33] T.W. Kahl, J.L. Kauschinger, E.B. Perry, Plastic Concrete Cut-Off Walls for Earth Dams, Technical Report REMR-GT-15, USACE, Vicksburg, MS, 1991.⟨https://apps.dtic.mil/sti/citations/ADA234566⟩.
[34] J. Kayser, T. Schulz, Spannungs-Verformungs-Verhalten erhärteter Bentonit-Zement-Suspensionen (in German), Bautechnik 76 (9) (1999) 747–756, https://doi.org/10.1002/bate.199904870.
[35] International Commission On Large Dams, Filling materials for watertight cut off walls, Bulletin 51 (1985).
[36] P. Zhang, Q. Guan, Q. Li, Mechanical properties of plastic concrete containing bentonite, research, J. Appl. Sci., Eng. Technol. 5 (4) (2013) 1317–1322.
[37] Comité Européen de Normalisation, EN 12390-13:2014-06 - Testing hardened concrete - Part 13: Determination of secant modulus of elasticity in compression (German version).2023.
[38] ASTM International, ASTM C469/C469M-14 - Test Method for Static Modulus of Elasticity and Poissons Ratio of Concrete in Compression.2023.
[39] Comité Européen de Normalisation, EN ISO 17892-7:2018–02 - Geotechnical investigation and testing – Laboratory testing of soil – Part 7: Unconfined compression test (German version).2023.
[40] ASTM International, ASTM D2166/D2166M-16 - Test Method for Unconfined Compressive Strength of Cohesive Soil.2023.
[41] Comité Européen de Normalisation EN 197–1:2011-11 - Cement - Part 1: Composition, specifications and conformity criteria for common cements (German version).2023.
[42] L.P. Meier, G. Kahr, Determination of the cation exchange capacity (CEC) of clay minerals using the complexes of Copper (II) ion with Triethylenetetramine and Tretraethylenepentamine, Clays Clay Miner. 47 (3) (1999) 386–388.
[43] A. Steudel, Selection strategy and modification of layer silicates for technical applications, Dissertation, Karlsr. Inst. Technol. (2009), https://doi.org/10.5445/KSP/1000010748.
[44] Deutsches Institut für Normung DIN 1045–2:2008–08 - Tragwerke aus Beton, Stahlbeton und Spannbeton - Teil 2: Beton - Festlegung, Eigenschaften, Herstellung und Konformität - Anwendungsregeln zu DIN EN 206–1 (in German).2023.
[45] Comité Européen de Normalisation EN 1008:2002–10 - Mixing water for concrete - Specification for sampling, testing and assessing the suitability of water, including water recovered from processes in the concrete industry, as mixing water for concrete (German version).2023.
[46] L. Lei, M. Palacios, J. Plank, A.A. Jeknavorian, Interaction between polycarboxylate superplasticizers and non-calcined clays and calcined clays: A review, Cem. Concr. Res. 154 (2022), 106717, https://doi.org/10.1016/j.cemconres.2022.106717.
[47] C.-S. Barbu, A.-D. Sabau, D.-M. Manoli, M.-S. Serbulea, Water/cement/bentonite ratio selection method for artificial groundwater barriers made of cutoff walls, Water 14 (3) (2022) 376, https://doi.org/10.3390/w14030376.
[48] Comité Européen de Normalisation EN 12350-2:2019-09 - Testing fresh concrete - Part 2: Slump test (German version).2023.
[49] Comité Européen de Normalisation EN 12350-5:2019-09 - Testing fresh concrete - Part 5: Flow table test (German version).2023.
[50] Comité Européen de Normalisation EN 12350-6:2019-09 - Testing fresh concrete - Part 6: Density (German version).2023.
[51] Comité Européen de Normalisation EN 12350-7:2019:09 - Testing fresh concrete - Part 7: Air content - Pressure methods (German version).2023.
[52] Comité Européen de Normalisation EN 12390-1:2021-09 - Testing hardened concrete - Part 1: Shape, dimensions and other requirements for specimens and moulds (German version).2023.

[53] Comité Européen de Normalisation EN 196-1:2016-11 - Methods of testing cement - Part 1: Determination of strength (German version).2023.
[54] Comité Européen de Normalisation EN 12390-2:2019-10 - Testing hardened concrete - Part 2: Making and curing specimens for strength tests (German version).2023.
[55] Comité Européen de Normalisation EN 12390-3:2009-07 - Testing hardened concrete - Part 3: Compressive strength of test specimens (German version).2023.
[56] Deutsches Institut für Normung DIN 4093:2015-11 - Bemessung von verfestigten Bodenkörpern - Hergestellt mit Düsenstrahl-, Deep-Mixing- oder Injektions-Verfahren (in German).2023.
[57] J.K. Norvell, J.G. Stewart, M.C. Juenger, D.W. Fowler, Influence of clays and clay-sized particles on concrete performance, J. Mater. Civ. Eng. 19 (12) (2007) 1053–1059, https://doi.org/10.1061/(ASCE)0899-1561(2007)19:12(1053).
[58] J. Ahmad, K.J. Kontoleon, M.Z. Al-Mulali, S. Shaik, M. HechmiElOuni, M.A. El-Shorbagy, Partial substitution of binding material by bentonite clay (BC) in concrete: a review, Buildings 12 (5) (2022) 634, https://doi.org/10.3390/buildings12050634.
[59] V.A. Fernandes, P. Purnell, G.T. Still, T.H. Thomas, The effect of clay content in sands used for cementitious materials in developing countries, Cem. Concr. Res. 37 (5) (2007) 751–758, https://doi.org/10.1016/j.cemconres.2006.10.016.
[60] B. Cao, J. Chen, A. Al-Tabbaa, Crack-resistant cement–bentonite cut-off wall materials incorporating superabsorbent polymers, Can. Geotech. J. 58 (6) (2021) 800–810, https://doi.org/10.1139/cgj-2020-0181.
[61] H. Zhao, Y. Ma, J. Zhang, Z. Hu, H. Li, Y. Wang, J. Liu, K. Wang, Effect of clay content on shrinkage of cementitious materials, Constr. Build. Mater. 322 (2022), 125959, https://doi.org/10.1016/j.conbuildmat.2021.125959.
[62] European Federation of Foundation Contractors. Deep Foundations Institute, Guide to Tremie Concrete for Deep Foundations, 2nd edition.,, 2018. ⟨https://www.effc.org/media_corner/effc-dfi-guide-to-tremie-concrete-for-deep-foundations-2nd-edition/⟩.
[63] G.A. Smith, S.W. Benham, A study of the flow-table and the slump test, Acids J. Proc. 27 (1) (1931) 420–438, https://doi.org/10.14359/8194.
[64] Deutsches Institut für Normung e.V., DIN-Fachbericht 100:2010–03 - Beton - Zusammenstellung von DIN EN 206–1 Beton - Teil 1: Festlegung, Eigenschaften, Herstellung und Konformität und DIN 1045–2 Tragwerke aus Beton, Stahlbeton und Spannbeton - Teil 2: Beton; Festlegung, Eigenschaften, Herstellung und Konformität; Anwendungsregeln zu DIN EN 206–1 (in German).2023.
[65] F. Jafarzadeh, S.H. Mousavi, Effect of specimenas age on mechanical properties of plastic concrete walls in dam foundations, Electron. J. Geotech. Eng. 17 (D) (2012) 473–482. ⟨http://www.ejge.com/2012/Abs12.042.htm⟩.
[66] H.S. Müller, M. Boumaaza, Modeling concrete properties: new approaches in MC2020, Struct. Concr. (2023), https://doi.org/10.1002/suco.202201231.
[67] D. AlósShepherd, S. Bruckschlögl, E. Kotan, F. Dehn, Untersuchungen zur Anwendbarkeit optischer Verformungsmessverfahren bei Plastic Concrete, Bautechnik 97 (3) (2020) 171–179, https://doi.org/10.1002/bate.201900071.